IAI Journals.ASM.org

Protective Role of Murine β-Defensins 3 and 4 and Cathelin-Related Antimicrobial Peptide in *Fusarium solani* Keratitis

Satya Sree N. Kolar, Hasna Baidouri, Samuel Hanlon, Alison M. McDermott

University of Houston, College of Optometry, Houston, Texas, USA

Antimicrobial peptides (AMPs), such as β-defensins and cathelicidins, are essential components of innate and adaptive immunity owing to their extensive multifunctional activities. However, their role in fungal infection *in vivo* remains elusive. In this study, we investigated the protective effect of murine β-defensin 3 (mBD3), mBD4, and the cathelicidin cathelin-related antimicrobial peptide (CRAMP) in a murine model of *Fusarium solani* keratitis. C57BL/6 mice showed significant corneal disease 1 and 3 days after infection, which was accompanied by enhanced expression of β-defensins and CRAMP. Disease severity was significantly improved 7 days after infection, at which time AMP expression was returning to baseline. Mice deficient in mBD3 (genetic knockout), mBD4 (short interfering RNA knockdown), or CRAMP (genetic knockout) exhibited enhanced disease severity and progression, increased neutrophil recruitment, and delayed pathogen elimination compared to controls. Taken together, these data suggest a vital role for AMPs in defense against *F. solani* keratitis, a potentially blinding corneal disease.

Fungal keratitis (keratomycosis), which is more common in warmer, humid climates, is a potentially devastating ocular infection. It is characterized by epithelial edema and intense stromal inflammation which, if untreated, can lead to corneal scarring, profound vision loss, and possibly endophthalmitis (1–3). While a range of fungi may be the culprit, *Fusarium* species are the most commonly isolated organisms, with *Fusarium solani* being implicated as the causative pathogen in more than 30% of cases (2–4). Ocular trauma and contact lens wear have long been recognized as the major predisposing factors for fungal keratitis, with *F. solani* being the culprit in the 2004-2006 worldwide epidemic associated with contact lens wear (5, 6). Little emphasis had been placed on the study of the host-pathogen response until quite recently. A breach in the corneal epithelium facilitates entry of conidia, which germinate, and the hyphae penetrate the corneal stroma, initiating an immune response mediated via toll-like receptors (TLRs) and Dectin-1 (7–10). Standard antifungal treatments are most effective if given early, but overall, fungal keratitis is notoriously difficult to treat, a problem further exacerbated by the appearance of drug-resistant strains (11, 12).

In an effort to offer novel interventional opportunities, it is imperative that we obtain a better understanding of the pathology, host response, and endogenous defense mechanisms related to *Fusarium*-induced keratitis. Antimicrobial peptides (AMPs), such as defensins and cathelicidin, are small cationic molecules with roles in pathogen killing, immunomodulation, and wound healing, among others (13, 14). Studies show that these endogenous molecules have potent antifungal activity, primarily via their membrane perturbation effects, but modulation of intracellular pathways may be involved (15–19). AMP immunomodulatory effects also raise the possibility of a protective effect without direct fungal killing (14, 20, 21).

Defensins and cathelicidin are produced by the ocular surface epithelia and by immune and inflammatory cells infiltrating the eye in response to infection (22). Recent *in vivo* studies in a murine model of bacterial keratitis have shown that deficiency (either by transient silencing by short interfering RNA [siRNA] or gene knockout [KO]) of mouse β-defensin 2 (mBD2) or mBD3 (homolog of human β-defensin 2) or the cathelicidin cathelin-related antimicrobial peptide (CRAMP) (homolog of human LL37) results in more severe infection and tissue damage (23–26). Further, exposure to *Candida albicans* significantly upregulated the expression of CRAMP (27), and mice deficient in CRAMP were more susceptible to *Candida* keratitis than wild-type (WT) mice (28). These studies show an essential role for AMPs in protection against *Pseudomonal* and *Candida* keratitis. However, despite being the most common cause of fungal keratitis, little is known about the role of AMPs in the innate immune response to *Fusarium*. Therefore, this study focused on establishing a role for mouse β-defensins and CRAMP in *F. solani*-induced keratitis *in vivo*.

MATERIALS AND METHODS

Fungi. *F. solani* (strain 36031; American Type Culture Collection, Manassas, VA), a strain capable of producing murine keratomycosis (29), was cultured in Sabouraud dextrose (SD) agar (Difco, Detroit, MI) for 3 days at 30°C. A colony of *F. solani* was inoculated into 4 ml of SD broth and grown aerobically overnight at 30°C, 250 rpm. Five hundred μl of fungal suspension was inoculated into 50 ml of fresh SD broth at 30°C, 250 rpm for 48 h to expand the culture. The conidia were harvested by filtering out the hyphae by passing the culture through sterile phosphate buffer (PB)-soaked gauze held in front of a 30-ml syringe. The turbidity of the suspension was adjusted to an optical density (OD) of 1 at 600 nm, which corresponds to 5×10^5 culturable units (CU) (30). The conidial suspension then was concentrated by centrifuging at $300 \times g$ for 10 min, resuspended in media to yield 1×10^6 CU/5 μl, and used to induce experimental keratomycosis in mice as described below.

Experimental animals. Inbred mixed-sex, age-matched, 6- to 8-week-old mice of the following genotypes were used: C57BL/6 mice (The Jackson Laboratory, Bar Harbor, ME), CRAMP KO mice ($Cnlp^{-/-}$) on the

Received 6 February 2013 Returned for modification 4 March 2013
Accepted 7 May 2013
Published ahead of print 13 May 2013
Editor: G. S. Deepe, Jr.
Address correspondence to Alison M. McDermott, amcdermott@optometry.uh.edu.

doi:10.1128/IAI.00179-13

C57 background (31), and homozygous WT (Defb3$^{+/+}$) and mBD3 KO (Defb3$^{-/-}$) mice on the C57 background that were custom generated by XenoGen Biosciences, now Taconic, Hudson, NY. Genotypes for Cnlp$^{-/-}$, WT, and KO mBD3 mice were confirmed by standard PCR analysis done on DNA isolated from tail clips. *In vivo* knockdown of mBD4 was achieved using a method previously described by Wu et al. using siRNA purchased from Santa Cruz Biotechnology (24). Briefly, 5 μl of 8 μM mBD4 siRNA or scrambled control siRNA was injected subconjunctivally into the right eye of C57BL/6 mice 1 day prior to fungal challenge. Topical application of 5 μl of 4 μM siRNA/mouse was performed once on the day of infection following fungal inoculation. The topical application was then repeated every 12 h for 2 days following infection. Silencing of mBD4 was confirmed by relative quantitative reverse transcription-PCR (RT-PCR) and immunostaining as described below. All protocols used were approved by the University of Houston Institutional Animal Care and Use Committee and were in compliance with the ARVO Statement for the Use of Animals in Ophthalmic and Vision Research.

Experimental keratomycosis. Wild-type and mutant mice were anesthetized by intraperitoneal injection of ketamine (100 mg/kg of body weight) and xylazine (10 mg/kg) (Vedco, Inc., St. Joseph, MO) and then placed beneath a surgical stereomicroscope. The cornea of the right eye was scratched with a sterile 27-gauge needle. Three parallel 1-mm scratches were made in the central cornea so as to abrade the full thickness of the epithelium and penetrate the superficial stroma. A 5-μl aliquot containing 1×10^6 CU of *F. solani* was pipetted directly onto the scarified cornea. The clinical progression of infection was monitored, and the extent of corneal damage was evaluated and documented by digital imaging using a slit lamp equipped with camera module CM 01 (Haag Streit USA, Mason, OH) at days 1, 3, and 7 postinfection (p.i.). The progression of infection was graded using a scale previously established by Wu et al. (30), where a grade of 0 to 4 is assigned for each of three criteria: area of opacity, density of opacity, and surface regularity. The scores from all three categories were summed to obtain a total possible score ranging from 0 to 12. A total score of 5 or less represented mild eye disease, 6 to 9 represented moderate disease, and more than 9 was categorized as severe disease.

Fungal load and myeloperoxidase assay. The fungal load was measured as previously described (32). Control and infected corneas from two to four mice were harvested at days 1, 3, and 7 p.i. and homogenized (8 to 10 strokes for 10 s, repeated 3 times until all tissue was uniformly homogenized) on ice in 1 ml of sterile phosphate-buffered saline (PBS), pH 7.4. A 100-μl aliquot of the homogenate was serially diluted in sterile PBS, and duplicate aliquots were plated onto SD agar plates, which were incubated for 48 to 72 h at 37°C, and then the number of culturable units was counted. The remaining homogenate was processed to quantitate the number of infiltrating neutrophils by myeloperoxidase (MPO) activity. MPO determination is a standard and well-established method for assessing neutrophil activity in infectious keratitis (33). To determine MPO activity, hexadecyltrimethylammonium bromide at a final concentration of 0.5% (wt/vol) in 50 mM phosphate buffer (pH 6.0) was added to 90 μl corneal homogenate. Samples were then freeze-thawed three times and centrifuged at 13,000 rpm for 20 min at 4°C. Ten μl of supernatant was pipetted in triplicate onto a microtiter plate, and the reaction was initiated by the addition of 90 μl 0.0167% (wt/vol) o-dianisidine dihydrochloride and 0.002% (vol/vol) H_2O_2 in PBS. The absorbance was measured for 90 min at 450 nm and plotted in comparison to a standard curve generated using purified MPO (Calbiochem, San Diego, CA) on the same plate (33). Results are expressed as relative units of MPO activity per cornea (1 MPO unit is proportional to 2×10^5 infiltrating neutrophils) (23, 24).

HRT imaging. Infected and control mouse corneas were imaged to obtain inflammatory cell counts using noninvasive corneal confocal microscopy. Mice were anesthetized as described above and then placed in an insulated 50-ml centrifuge tube with the bottom cut out to allow the mouse head to protrude for imaging. Eyes were applanated and scanned using a Heidelberg retinal tomographer III with a Rostock cornea module (HRT-RCM) (400- by 400-μm resolution). The mouse holding tube was attached to a gooseneck clamp and positioned such that the surface of the objective cap was perpendicular to the surface normal of the corneal apex. The cornea was applanated with enough force to maintain a stable image. Full-thickness volume scans were obtained from multiple locations within the central cornea. The bright, small, light-reflective cells indicate inflammatory cell (most likely neutrophil) infiltration of the infected cornea, as demonstrated by other investigators (34). Inflammatory cells were counted using Image J software (NIH).

TABLE 1 Primer sequences

Primer	Direction	Sequence (5′ to 3′)
mBD1	Forward	CTGGGAGTTTCACATCCTCTC
	Reverse	CTCCATGTTGAAGGCATTTGT
mBD2	Forward	CTACCAGCCATGAGGACTCTC
	Reverse	GTACTTGCAACAGGGGTTCTT
mBD3	Forward	GGATCCATTACCTTCTGTTTGC
	Reverse	ATTTGAGGAAAGGAACTCCAC
mBD4	Forward	GCTTCAGTCATGAGGATCCAT
	Reverse	CTTGCTGGTTCTTCGTCTTTT
mBD5	Forward	CCTTCTCTTTGCATTTCTCCT
	Reverse	TTTCTCTTGCAGCAGTTGAGA
mBD6	Forward	TACCTGCTCTTTGCCTTTATCC
	Reverse	TTCTGGCACTTATTCACATTGC
mBD14	Forward	TCTTGTTCTTGGTGCCTGCT
	Reverse	CGACCGCTATTAGAACATCGAC
CRAMP	Forward	GCCGCTGATTCTTTTGACAT
	Reverse	GCCAAGGCAGGCCTACTACT
RPII	Forward	CTACACCACCTACAGCCTCCAG
	Reverse	TTCAGATGAGGTCCATGAGGAT

Quantitative real-time PCR. Whole corneas from infected and control eyes ($n = 8$ mice/group/time point) were harvested and pooled in RNA lysis buffer at days 1, 3, and 7 p.i. In preliminary experiments, attempts were made to isolate epithelium only. However, due to a very robust infection leading to compromise of the cornea and sometimes perforation, we had to abandon this approach and harvest whole corneas for the experiments. Total RNA was extracted using a Totally RNA total cellular RNA kit from Applied Biosystems (Carlsbad, CA) and quantified using a NanoDrop 2000 spectrophotometer (Thermo Scientific, Wilmington, DE). To degrade any contaminating DNA, all samples were treated with DNase (Qiagen, Valencia, CA). Two μg of total RNA was reverse transcribed to cDNA using Moloney murine leukemia virus reverse transcriptase. The 20-μl reaction mixture contained 100 U reverse transcriptase, 10 U RNasin, 1 μg of oligo(dT) primers, 10 mM deoxynucleoside triphosphates (dNTPs), and reaction buffer (Biochain Institute Inc., Newark, CA). Relative quantitative real-time PCR amplification was performed using SYBR green quantitative PCR Mastermix kits (Stratagene, Santa Clara, CA) with specific primers at a concentration of 10 μM (sequences are presented in Table 1) at optimized concentrations to evaluate the expression of mouse defensins (mBD1, mBD2, mBD3, mBD4, mBD5, mBD6, and mBD14) and CRAMP. The PCR included an initial 10-min denaturation at 95°C. Amplification of the cDNA was performed for 40 cycles: denaturation, 95°C for 30 s; annealing, 56°C for 1 min; and extension, 72°C for 30 s. No-RT and no-template controls were included. Data analysis was performed using the Stratagene Mx3005 software, and disassociation melt curves were analyzed to ensure reaction specificity. Amplified gene products were normalized to RNA polymerase II (RPII), the internal control, and calibrated to uninfected day 0 samples.

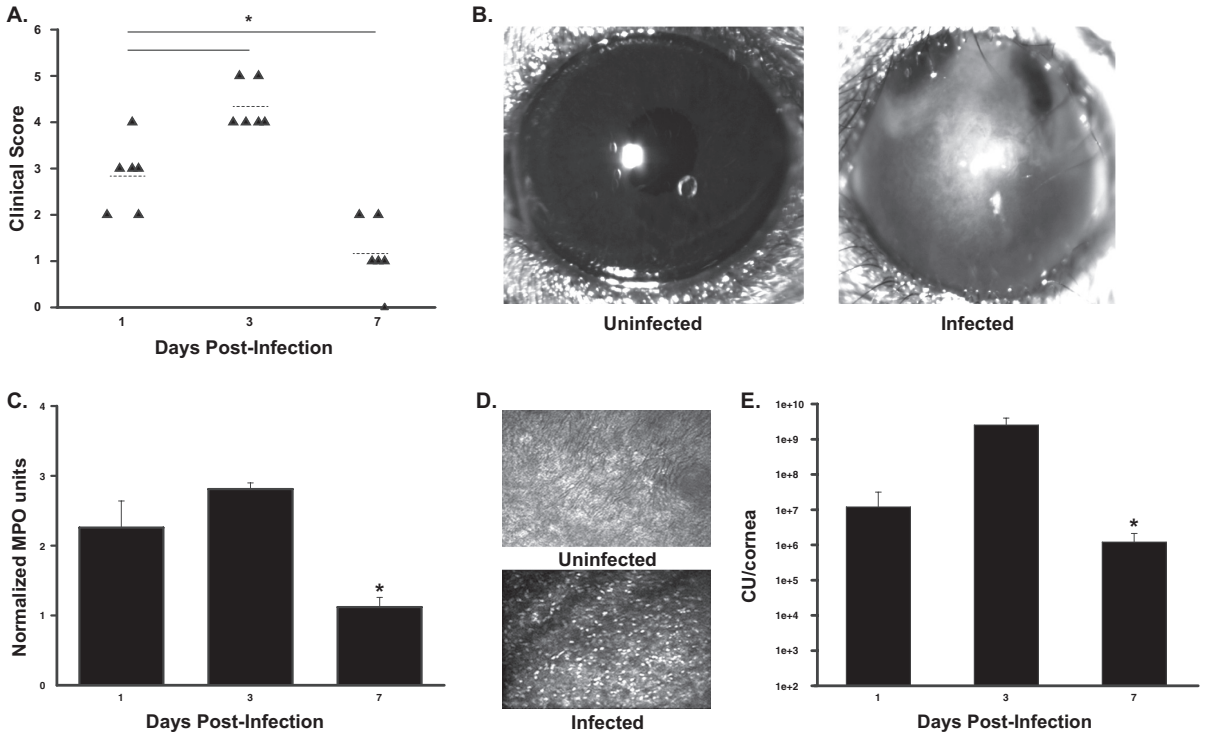

FIG 1 *F. solani* keratitis in C57BL/6 mice. (A) Clinical scores indicate marked corneal disease at days 1 and 3 p.i. with an improvement at day 7 p.i. Data are scores from individual mice in one experiment, which was repeated 5 times with comparable results. The short horizontal dashed lines represent the mean clinical score. (B) Representative photographs taken with a slit lamp at day 3 p.i. depict a significant inflammatory response in the infected cornea compared to the uninfected control. Neutrophil recruitment, as indicated by MPO activity ($n = 5$) and representative HRT images (at day 3 p.i.), are shown in panels C and D, respectively. (E) Viable fungal load ($n = 5$) quantifying *F. solani* culturable units (CU). Data for panels C and E are from a representative experiment, which was repeated 3 times with comparable results (an asterisk indicates significant difference; $P \leq 0.05$).

Immunostaining. Uninfected control and infected eyes were enucleated on days 1, 3, and 7 p.i. ($n = 3$/group/time). The globe was rinsed in sterile Dulbecco's PBS, embedded in Tissue-Tek optimal cutting temperature compound (Miles Inc., Naperville, IL), and immediately frozen in liquid nitrogen. Ten-micrometer-thick sagittal sections were cut and fixed in ice-cold acetone for 3 min. The slides were rinsed in cold PBS and blocked with 5% bovine serum albumin, 1% fish gelatin, 10% normal goat serum, and 0.1% Triton X-100 in PBS at room temperature for 2 h. Sections were then incubated with primary antibodies against CRAMP, mBD3, or mBD4 (Santa Cruz Biotechnology, Santa Cruz, CA) diluted 1/50 in blocking buffer overnight at 4°C. The sections were then rinsed 3 times in PBS and blocked at room temperature for 30 min. The tissue was then incubated with goat anti-rabbit IgG coupled to Alexa Fluor 546 (Invitrogen, Carlsbad, CA), diluted 1/400 in blocking buffer, for 60 min at room temperature. Control sections were similarly treated, but the primary antibodies were replaced with rabbit IgG (R&D systems, Minneapolis, MN). Vectashield prolong gold mounting medium (Vector Laboratories, Burlingame, CA) was used to mount the coverslips, staining was visualized using a DeltaVision Core inverted microscope (Applied Precision, Issaquah, WA) system, and images were processed using SoftWorx software.

Statistical analysis. Multiple comparisons were made using analysis of variance (ANOVA) in conjunction with a Tukey's honestly significant difference (HSD) test to report mean differences. All experiments were repeated at least three times, except where stated, to ensure reproducibility.

RESULTS

***F. solani* keratitis in C57BL/6 mice.** Clinical progression of infection, neutrophil recruitment, and fungal load were examined in WT C57BL/6 mice infected with *F. solani*. Fig. 1A shows the mean clinical scores from mice ($n = 6$) examined by a slit lamp. At day 1 p.i., the corneas appeared cloudy with mild surface irregularity and an area of opacity ranging from 25 to 50%, with a mean clinical score of 2.83 ± 0.30. Fig. 1B shows an uninfected eye and the typical appearance of *F. solani* corneal infection seen at day 3 p.i. At this time point, the cornea was cloudy with significant edema, and there were dense infiltrates and a nonuniform opacity covering about 50 to 75% of the cornea. At day 3 p.i., the mean clinical score of 4.33 ± 0.21 was significantly higher than that at day 1 p.i. ($P \leq 0.002$). Seven days following fungal challenge with *F. solani*, the signs of inflammation receded and there was improvement in the corneal condition, with the mean clinical score of 1.16 ± 0.3 tending toward the baseline. The mean clinical scores of the infected eyes at day 7 p.i. were significantly lower than at days 1 and 3 p.i. ($P \leq 0.003$).

The number of neutrophils recruited to the site of infection was determined by measuring the relative MPO activity in isolated corneas (Fig. 1C). MPO activity was readily apparent by day 1 p.i. and peaked at day 3 p.i. In keeping with the improved clinical score (Fig. 1A) at day 7 p.i., MPO activity was virtually undetectable above the background (which was normalized to 1). In addition to MPO assays, corneal confocal microscopy, a novel noninvasive technique, was used to provide *in vivo* imaging of the infiltrating cells in the cornea. Images (Fig. 1D) were collected at a depth half the thickness of the cornea. The infiltrating cells were visible as small, highly reflective, roughly circular cells, character-

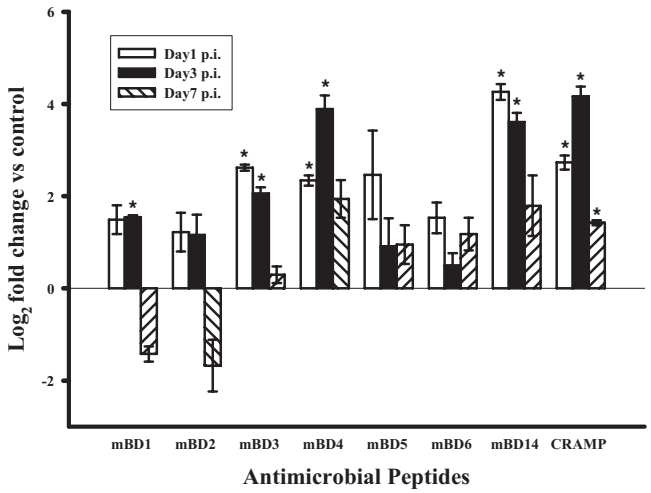

FIG 2 AMP mRNA is upregulated in *F. solani* keratitis in C57BL/6 mice. mRNA levels for all AMPs tested showed upregulation at day 1 and/or 3 compared to uninfected controls. Data are means ± standard errors of the means (SEM) and are representative of three individual experiments (an asterisk indicates significant difference; $P \leq 0.05$).

istic of neutrophils (34), and were present in large numbers at days 1 (not shown) and 3 p.i. but were undetectable by day 7 p.i. (not shown) and in uninfected controls. At day 3 p.i., corneas from *F. solani*-infected right eyes demonstrated a count of 263 ± 32 inflammatory cells per 400- by 400-μm field at a midsection plane, while the uninfected control eye showed no infiltration. Viable fungal load was determined by quantifying *F. solani* colonies at days 1, 3, and 7 p.i. As shown in Fig. 1E, levels of recoverable viable fungi were high at days 1 and 3 p.i. However, 7 days following fusarium challenge, the pathogen load decreased significantly. These data were consistent with the aforementioned clinical grading and MPO data demonstrating worsening of infection over 3 days followed by recovery. Preliminary experiments comparing clinical score, MPO assay, and viable fungal counts showed no significant difference among a scratched but not infected group of animals and nonscratched and noninfected controls (data not shown).

Antimicrobial peptide expression following *F. solani* infection. Relative quantitative RT-PCR and immunostaining were used to determine mRNA and protein expression of selected murine AMPs following fungal challenge. As shown in Fig. 2, there was an upregulation of all AMPs tested at day 1 and/or 3 p.i. compared to the uninfected controls. mBD3, mBD5, mBD6, and mBD14 mRNA levels peaked at day 1, and those of mBD1 and mBD2 were similar at days 1 and 3 p.i. The expression levels of mBD4 and CRAMP peaked at day 3, and all of the genes tended to the baseline at day 7. The expression levels of CRAMP and mBD14 were significantly notable; at their peak, they were 4.17 ± 0.21 and 4.26 ± 0.17 $\log_2$ fold higher than those of the controls ($P < 0.04$ and $P < 0.006$, respectively). Despite the significant increase in mBD14, further exploration into its effect was not feasible due to the lack of gene specific reagents. However, having shown significant upregulation of mBD3 (peak 2.62 ± 0.07 $\log_2$ fold increase compared to the control on day 1 p.i.; $P < 0.0003$), mBD4 (peak 3.89 ± 0.29 $\log_2$ fold increase compared to the control on day 3 p.i.; $P < 0.002$), and CRAMP mRNA based on reagent availability and mutant mouse resources, we further investigated these specific AMPs.

Protein expression of mBD3, mBD4, and CRAMP was examined in corneal sections using immunofluorescent staining. As shown in Fig. 3, there was minimal to no staining in uninfected corneas for mBD3 and mBD4. However, data demonstrated that there was basal expression seen for CRAMP. At days 1 and 3 p.i., mBD3, mBD4, and CRAMP showed a more intense staining in the infected corneal epithelium (Fig. 3). At day 7 p.i., there was no difference seen in the intensity of staining of infected versus control corneas (Fig. 3). These data paralleled the mRNA expression pattern seen in Fig. 2.

Involvement of mBD3 in *F. solani* keratitis. mBD3 KO and age-matched littermate WT mice were used to investigate the role of mBD3 in the ocular defense mechanism against *F. solani* infection. As shown in Fig. 4, mBD3 KO mice exhibited enhanced severity of disease compared to their WT controls. At day 1 p.i., infected WT mice demonstrated a cloudy cornea with an intact pupillary margin, mild edema, and about 30 to 40% corneal opacity. In comparison, the infected corneas of KO mice displayed a significantly uniform cloudiness and edema with a uniform opacity covering more than 60% of the central cornea. The mean clinical score was 3.0 ± 0.31 and 4.5 ± 0.64 at day 1 p.i. for WT and mBD3 KO mice, respectively, although this difference did not reach statistical significance ($P < 0.06$). The progression of infection was significantly greater in the mBD3 KO than the WT animals, with the KO mice demonstrating a much more severe corneal response at day 3 p.i. At this time point, the mean clinical score of the WT mice, which was 4.40 ± 0.24, was significantly lower than that of the mBD3 KO mice, with a score of 6.75 ± 0.48 ($P < 0.005$). At day 7 p.i., the disease showed significant improvement in the WT animals (clinical score of 1.2 ± 0.37), but corneas of the KO mice worsened (clinical score, 8.75 ± 0.94; $P < 0.0005$

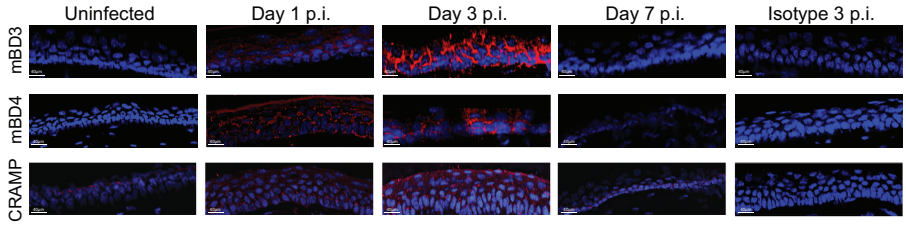

FIG 3 Elevated AMP protein expression in *F. solani* keratitis in C57BL/6 mice. Immunostaining revealed increased mBD3, mBD4, and CRAMP at days 1 and 3 p.i. compared to uninfected control corneas. Representative images of isotype controls at day 3 p.i. using primary host IgG showed no immunopositive staining. AMP-specific staining is shown in red, and DAPI was used to stain the nuclei. All images were taken at ×200 magnification. Scale bars represent 40 μm. Images are representative of data from 3 mice per group. The experiment was repeated two times with comparable results.

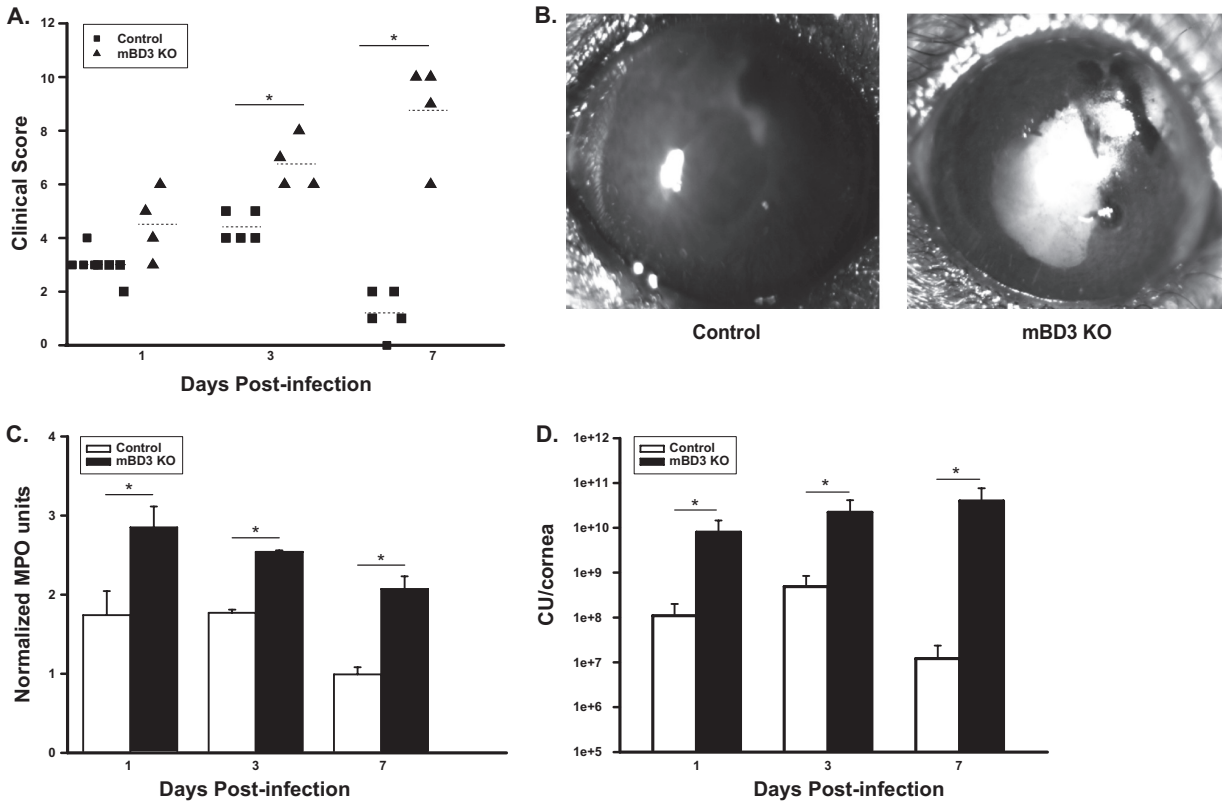

FIG 4 Involvement of mBD3 in *F. solani* keratitis. (A) Clinical scores indicated that infected mBD3 KO mice demonstrated a more severe disease and no recovery compared to the WT controls. The short horizontal dashed lines represent the mean clinical score. (B) Representative photographs of infected mBD3 KO and WT controls at day 3 p.i. (C) MPO activity revealed a significantly greater neutrophil recruitment in infected KO than in control animals ($n = 4$). (D) Viable fungal load was significantly greater in the infected KO mice than in the controls ($n = 4$). Data are from a representative experiment, which was repeated twice with comparable results (an asterisk indicates significant difference; $P \leq 0.05$).

compared to the WT), demonstrating significant corneal edema and descemetocele formation, leading to perforation in some corneas. The KO animals had a higher mean clinical score at day 7 than at day 1 p.i. ($P < 0.01$). The scores for the KO mice were not significantly different between days 3 and 7 p.i. ($P < 0.10$). This was in contrast to the mBD3 WT animals, which showed recovery from the infection at day 7 p.i. compared to day 1 p.i. ($P < 0.01$) and day 3 p.i. ($P < 0.0005$). Fig. 4B shows representative photographs of mBD3 WT- and KO-infected corneas at day 3 p.i. MPO activity and plate counts were used to determine neutrophil recruitment and viable fungal cells in the WT- and mBD3 KO-infected corneas. Data in Fig. 4C and D demonstrate that compared to the WT, mBD3 KO animals had increased MPO activity and an enhanced fungal load at days 1, 3, and 7 p.i.

Silencing of mBD4 and its effect on disease progression. As there is no mBD4 knockout mouse line available, to examine the role of this AMP in the progression of *F. solani* keratitis *in vivo*, knockdown using siRNA was performed in C57BL/6 mice as described by Wu et al. (24). Relative quantitative RT-PCR and immunostaining were performed at 3 days p.i. to confirm knockdown. As shown in Fig. 5A, at this time there was a significant decrease, of approximately 60%, in mBD4 mRNA expression compared to that of untreated controls and a nonspecific scrambled siRNA control. There was no significant difference between the untreated and scrambled siRNA-treated animals. Immunofluorescence staining 3 days p.i. also indicated a marked decrease in mBD4 protein in specific siRNA-treated eyes compared to scrambled siRNA and untreated controls (Fig. 5B).

The next set of experiments was designed to determine if knockdown of mBD4 had a significant impact on disease severity. The results (Fig. 6) indicated that siRNA-treated mice had more severe signs of corneal disease than the scrambled siRNA-treated and untreated infected controls at days 1 and 3 p.i. As shown in Fig. 6A, the clinical score at day 1 p.i. for mBD4 knockdown animals (6.67 ± 0.21) was significantly greater than that for scrambled siRNA (3.33 ± 0.49; $P < 0.0001$) or untreated infected controls (3.83 ± 0.60; $P < 0.0003$). The clinical scores at day 3 p.i. reflect severe disease progression in the mBD4 siRNA-treated animals (10.87 ± 0.48) compared to their scrambled (5.83 ± 0.70; $P < 0.0002$) and untreated infected controls (4.67 ± 0.80; $P < 0.0005$). Fig. 6B shows representative photographs of control, scrambled siRNA- and mBD4 siRNA-treated mice at day 3 p.i. Corneas in the mBD4 knockdown mice exhibited a uniform opacity covering the entire cornea with significant edema, descemetocele formation, and corneal perforation in some animals, indicating very severe corneal disease. There was no significant difference in clinical score among scrambled and untreated control animals at day 1 ($P < 0.83$) or 3 p.i. ($P < 0.30$). As shown in Fig. 6C, there was significantly higher neutrophil recruitment in the mBD4 siRNA-treated corneas than in the scrambled siRNA and untreated infected control corneas ($P < 0.02$). MPO values in in-

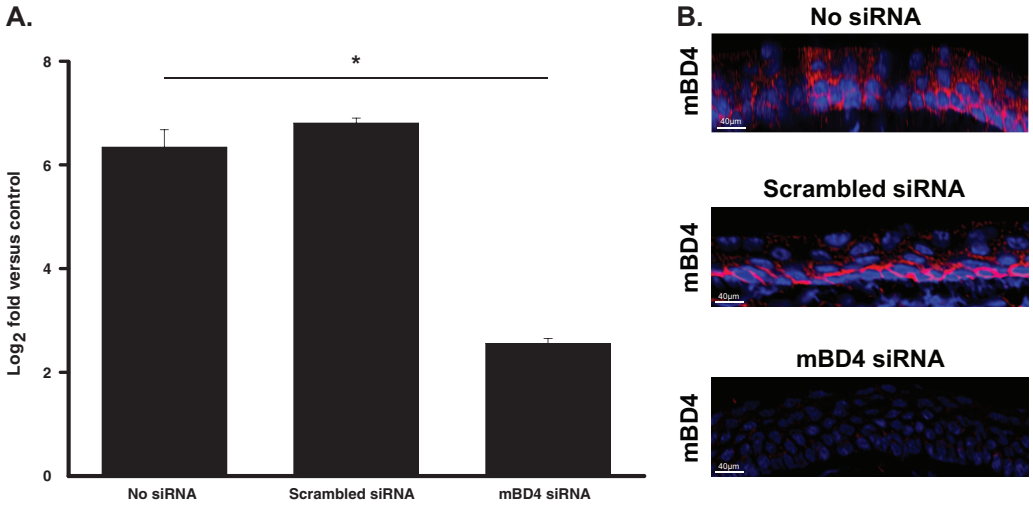

FIG 5 Evidence of mBD4 knockdown. (A) RT-PCR to confirm *in vivo* silencing of the mBD4 gene at day 3 p.i. Data are expressed as log fold change versus the control ± SEM from a representative experiment ($n = 5$), repeated 3 times with reproducible results (an asterisk indicates significant difference; $P \leq 0.05$). (B) Immunostaining indicated a significant decrease in protein expression of mBD4 in siRNA-treated animals compared to the infected scrambled siRNA-treated or untreated infected controls. AMP-specific staining is shown in red, and DAPI was used to stain the nuclei. Images are representative of sections from an experiment with 5 mice per group. The experiment was repeated 2 times with comparable results. All images were taken at ×200 magnification. Scale bars represent 40 μm.

fected corneas of scrambled siRNA- and no-siRNA-treated mice showed no significant difference ($P < 0.15$). Similarly, the data in Fig. 6D show that the fungal load in mBD4 siRNA-treated mice was significantly higher than that in the scrambled siRNA-treated and untreated infected control animals ($P < 0.03$). We did not investigate time points longer than 3 days, as the knockdown was effective and, as detailed above, there was a marked difference among control and treated animals.

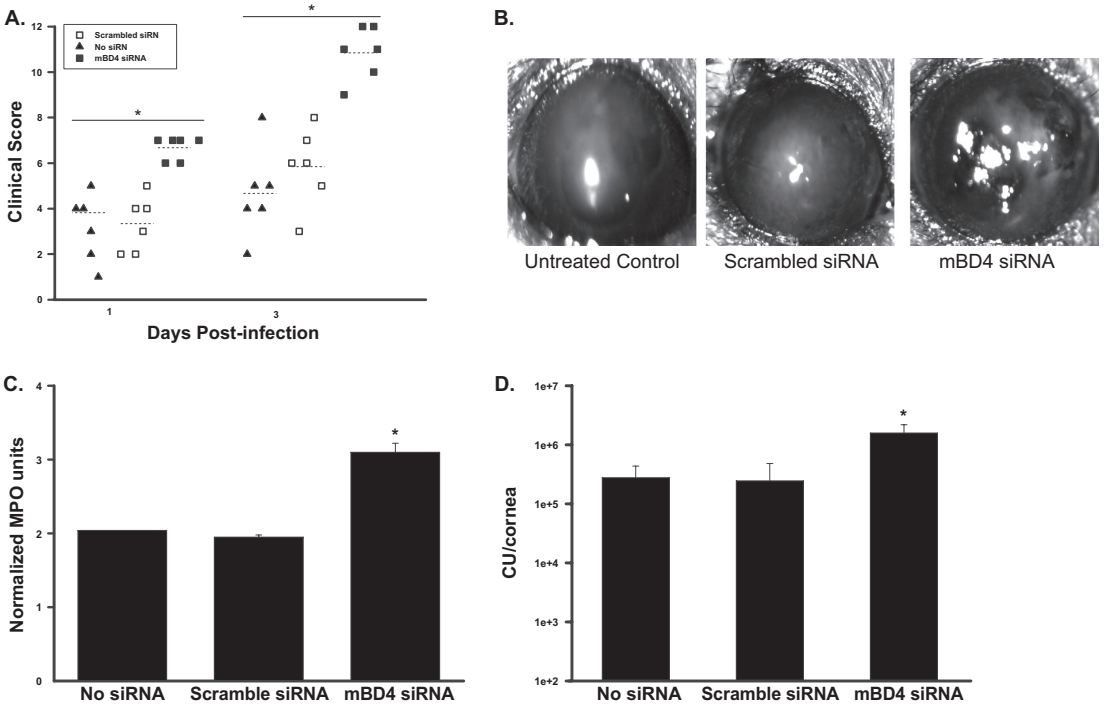

FIG 6 Knockdown of mBD4 increases disease severity. (A) *In vivo* silencing of mBD4 resulted in an increase in the mean clinical score in *F. solani*-infected corneas compared to corneas treated with a scrambled siRNA and untreated controls. The short horizontal dashed lines represent the mean clinical scores. (B) Representative photographs taken at day 3 p.i. of mBD4 siRNA-treated, scrambled siRNA-treated, and untreated infected control animals. (C) Neutrophil recruitment at day 3 p.i. as determined by MPO assay ($n = 5$). (D) Viable fungal load at day 3 p.i. ($n = 5$). Data are from a representative experiment, which was repeated 3 times with comparable results (an asterisk indicates significant difference; $P \leq 0.05$).

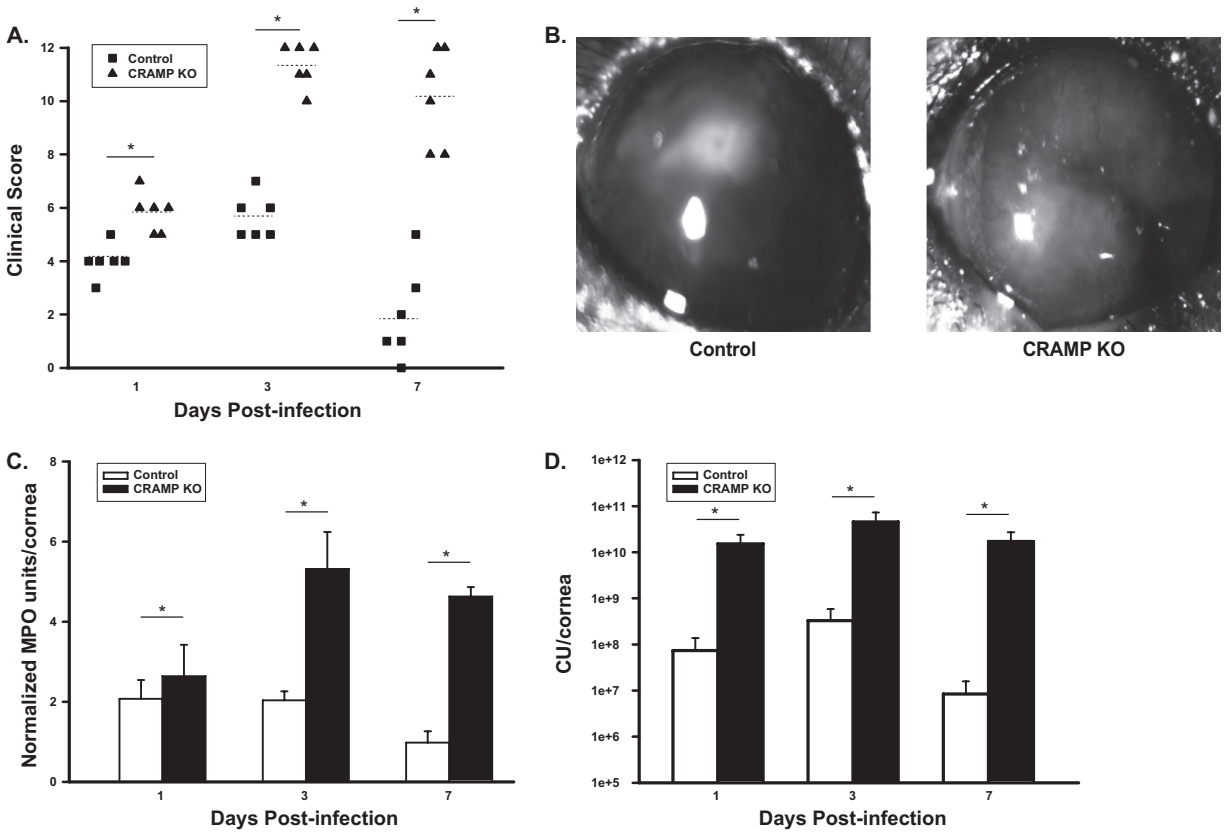

FIG 7 Involvement of CRAMP in *F. solani* keratitis. (A) Clinical scores indicated that infected CRAMP KO mice had more severe disease and no recovery compared to controls. The short horizontal dashed lines represent the mean clinical scores. (B) Representative photographs of the infected eye for CRAMP KO and control at day 3 p.i. (C) Neutrophil recruitment as determined by MPO assay ($n = 5$). (D) Viable fungal load ($n = 5$). Data are from a representative experiment, which was repeated 3 times with comparable results (an asterisk indicates significant difference; $P \leq 0.05$).

Involvement of CRAMP in *F. solani* keratitis. To investigate if the induction of CRAMP expression seen in response to fungal challenge was of significance in limiting the severity of the infection, keratitis was compared among CRAMP KO and C57BL/6 control mice. At day 1 p.i., the C57BL/6 mice demonstrated a central corneal opacity occupying about 30% of the cornea, with mild swelling and surface irregularity not seen in to the KO mice. The mean clinical score of the KO mice (5.83 ± 0.28) was significantly greater ($P < 0.005$) than that of C57BL/6 mice (4.17 ± 0.24). At 3 days p.i., the severity of disease was progressive in both C57BL/6 control and KO mice. However, the disease progressed much more rapidly in the KO mice, which exhibited a clinical score of 11.33 ± 0.30 compared to a much milder increase to a clinical score of 5.67 ± 0.20 in the control mice ($P < 0.001$). At 7 days p.i., clinical scores for the CRAMP-KO mice remained significantly elevated, while the infected corneas of the control mice showed marked signs of improvement and disease resolution. At this time, the mean clinical scores were statistically significantly different, with values of 1.83 ± 0.64 and 10.17 ± 0.68 for control and KO mice, respectively ($P < 0.0001$). Representative photographs of infected corneas of C57BL/6 control and CRAMP KO mice at day 3 p.i. are shown in Fig. 7B. The number of neutrophils recruited and fungal load were determined on days 1, 3, and 7 p.i. As shown in Fig. 7C, CRAMP KO mice had greater neutrophil recruitment than their infected controls at all three time points, with the MPO activity on days 1, 3, and 7 p.i. being significantly higher in the KO mice ($P < 0.04$). Fig. 7D shows that the KO mice exhibited a statistically significant higher fungal load at days 1, 3, and 7 p.i. ($P < 0.05$, $P < 0.02$, and $P < 0.01$, respectively).

DISCUSSION

In this investigation, we used a mouse model to study AMPs in fungal keratitis, and in doing we so revealed an indispensable role for mBD3, mBD4, and CRAMP in defense against *F. solani*-induced keratitis. Our study showed that in C57BL/6 mice, *F. solani* induced mild to moderate keratitis accompanied by neutrophil recruitment, as demonstrated by increased MPO activity and HRT imaging. Evidence from earlier studies by Wu et al. demonstrated histopathological evidence in the mouse model that corneal invasion by fungal hyphae was associated with enhanced neutrophil recruitment (35). Additionally, Karthikeyan et al. studied cell morphology in fusarium keratitis in human corneas and showed that the majority (95%) of infiltrating cells were neutrophils (9). Therefore, although MPO activity is not neutrophil specific, these earlier studies indicate that in fungal keratitis the major infiltrating inflammatory cells are neutrophils; thus, in our study, the observed MPO activity could be attributed primarily to neutrophils. Further support comes from our HRT imaging. While HRT cannot conclusively distinguish inflammatory cell subtypes, the size, morphology, and reflectance of the infiltrating cells were also suggestive of a predominantly neutrophilic infiltration. The C57BL/6 mice were able to resolve the infection, clear the cornea

of inflammatory cells, and restore corneal integrity within 7 days after fungal inoculation. This pattern of disease progression and recovery within 7 to 14 days following fungal inoculation is comparable to that seen in other studies using various fungi as the infecting agent in immunocompetent mice (27, 36).

AMP mRNA expression paralleled the clinical course of infection, with all of the β-defensins tested and CRAMP being elevated at 1 and 3 days p.i. and tending toward baseline by day 7 p.i. Reliable protein detection reagents are not available for all of the AMPs we tested, but we were able to confirm the same pattern of expression for mBD3, mBD4, and CRAMP proteins, giving the first indication that β-defensins and CRAMP are important for defense against *F. solani* infection. In contrast to our findings with *F. solani*, in a recent study by Yuan et al., who used *C. albicans* as the infecting agent, the authors studied expression of multiple AMPs but observed an increase only in CRAMP, suggesting differences in the ability of these two pathogens to modulate AMP expression (27). It is also possible that the difference can be attributed to the mouse strains used, as disparate regulation of defensin expression has been reported among BALB/c and C57BL/6 mice in a bacterial keratitis model (24). Owing to the infection-induced damage, we were unable to separate epithelium from the rest of the cornea to a degree suitable for sensitive RT-PCR analysis, limiting our ability to determine the cellular sources of AMP mRNA expression (lack of reliable reagents for protein detection of several murine AMPs also precluded detection by immunostaining). Mouse neutrophils express high levels of CRAMP (31), and we found marked expression of mBD1 but not other defensins by murine neutrophils and macrophages (S. S. Kolar, H. Baidouri, W. Zhang, and A. M. McDermott, presented at the 6th International Conference on the Tear Film and Ocular Surface, Florence, Italy, 23 to 25 September 2010). This suggests that infiltrating inflammatory cells contribute to the upregulation of mBD1 (not pursued due to the current lack of evidence of its antifungal activity against *F. solani*) and CRAMP that we observed, but not to that of mBD2 to mBD6 and mBD14. However, we cannot exclude the possibility that the environment within the fungus-infected cornea upregulated inflammatory cell expression of other AMPs. The advent of improved reagents for AMP protein detection will help shed light on this.

In order to provide firm evidence of involvement of AMPs in defense against fungal keratitis, we took advantage of the availability of two AMP knockout strains and a previously published and proven method to knock down β-defensin expression by siRNA (24, 25). We obtained approximately 60% mBD4 gene knockdown, which is comparable to that observed by Wu et al. (24), and more significantly, we were not able to detect any mBD4 peptide by immunostaining. In stark contrast to the control mice, the mBD3 and CRAMP KO mice and mBD4 knockdown mice all demonstrated much more severe disease with no recovery. The KO and knockdown mice also showed greater neutrophil recruitment than control mice. This may be expected to benefit fungal clearance; however, this was not the case, as KO and knockdown animals demonstrated suboptimal fungal clearance resulting in an increased fungal load compared to the controls. Thus, despite the presence of additional neutrophils in the animals, the absence of specific AMPs compromises the ability of the immune response to kill fusarium. Also, both enhanced neutrophil recruitment and compromised fungal clearance likely contribute to the increased disease severity in the KO and knockdown animals. Taken together, our data suggest that mBD3, mBD4, and CRAMP play a critical role in defense against *F. solani*. Furthermore, our findings are in agreement with those of Gao et al. (28), who showed that CRAMP KO mice were susceptible and had severe disease in response to corneal infection with another fungal pathogen, *C. albicans*.

As noted earlier, AMPs are known for both direct killing abilities and immunoregulatory actions (13, 14). However, it is unclear if our finding of AMPs having a protective role against fungal keratitis is the result of direct fungal killing or the result of immunomodulatory activities, or if it is a net result of both of these factors. A few studies have confirmed direct antifungal activity for some of the AMPs we investigated, including mBD3 and CRAMP (18, 37, 38). Thus, direct killing is likely to be an important mechanism contributing to AMP protective effects in fungal keratitis. AMPs such as CRAMP have been reported to be chemotactic for some immune and inflammatory cells, including neutrophils (39). However, in our model, this effect appears to have little impact, as CRAMP KO mice had significantly greater neutrophil recruitment than controls, suggesting that other chemoattractants, such as keratinocyte chemoattractant (KC), have much greater influence. That the relative importance of chemoattractants may be altered in the KO animals should also be acknowledged. Other immunomodulatory actions that may be of significance are currently being investigated in our laboratory.

A particularly interesting finding from our study is that lack of any of the AMPs we tested was sufficient to result in very severe infection. Thus, for example, despite having normal CRAMP and mBD3, mBD4 knockdown animals were unable to resolve the infection. This is suggestive of a combinatorial effect between these AMPs. In conclusion, while the actual mechanisms have yet to be elucidated, this investigation provides direct *in vivo* evidence that the endogenously expressed β-defensins mBD3 and mBD4 and the cathelicidin CRAMP play a significant role in the host defense response to *F. solani*-induced keratitis. Furthermore, these data provide insight into disease pathogenesis in addition to opening up new opportunities for development of AMP-based therapeutics for the treatment of ocular diseases such as *F. solani* keratitis.

ACKNOWLEDGMENTS

This work was supported by NIH EY13175 (A.M.M.), University of Houston College of Optometry (UHCO) Vision Grant to Advance Research (A.M.M.), and NIH EY07551 (UHCO core grant).

We gratefully acknowledge Richard Gallo (UC San Diego) for donating the CRAMP antibody and granting permission for the use of the CRAMP KO mice in a C57BL/6 background, which were kindly provided by Fu Shin Yu (Wayne State University).

We thank Russell Lewis, Alan Burns, Ronald Harwerth, and Rachel Redfern (all at the University of Houston) for their helpful discussions, technical advice, and use of the DeltaVision microscope (A.B.) and HRT equipment (R.H.).

We have no conflicts of interest to declare.

REFERENCES

1. **Alfonso EC, Galor A, Miller D.** 2010. Fungal keratitis in cornea, p 1009–1022. *In* Krachmer JH, Mannis MJ, Holland EH (ed), Cornea: fundamentals in cornea and external disease. Elsevier Mosby, Maryland Heights, MD.
2. **Gopinathan U, Sharma S, Garg P, Rao GN.** 2009. Review of epidemiological features, microbiological diagnosis and treatment outcome of microbial keratitis: experience of over a decade. Indian J. Ophthalmol. **57:** 273–279.

3. **Sirikul T, Prabriputaloong T, Smathivat A, Chuck RS, Vongthongsri A.** 2008. Predisposing factors and etiologic diagnosis of ulcerative keratitis. Cornea **27:**283–287.
4. **Wang L, Sun S, Jing Y, Han L, Zhang H, Yue J.** 2009. Spectrum of fungal keratitis in central China. Clin. Exp. Ophthalmol. **37:**763–771.
5. **Gaujoux T, Chatel MA, Chaumeil C, Laroche L, Borderie VM.** 2008. Outbreak of contact lens-related *Fusarium* keratitis in France. Cornea **27:**1018–1021.
6. **Patel A, Hammersmith K.** 2008. Contact lens-related microbial keratitis: recent outbreaks. Curr. Opin. Ophthalmol. **19:**302–306.
7. **Thomas PA.** 2003. Fungal infections of the cornea. Eye **17:**852–862.
8. **Zhong WX, Sun SY, Zhao J, Shi WY, Xie LX.** 2007. Retrospective study of suppurative keratitis in 1054 patients. Zhonghua Yan Ke Za Zhi **43:**245–250.
9. **Karthikeyan RS, Leal SM, Jr, Prajna NV, Dharmalingam K, Geiser DM, Pearlman E, Lalitha P.** 2011. Expression of innate and adaptive immune mediators in human corneal tissue infected with *Aspergillus* or *Fusarium*. J. Infect. Dis. **204:**942–950.
10. **Leal SM, Jr, Pearlman E.** 2012. The role of cytokines and pathogen recognition molecules in fungal keratitis–insights from human disease and animal models. Cytokine **58:**107–111.
11. **Jurkunas UV, Langston DP, Colby K.** 2007. Use of voriconazole in the treatment of fungal keratitis. Int. Ophthalmol. Clin. **47:**47–59.
12. **Edelstein SL, Akduman L, Durham BH, Fothergill AW, Hsu HY.** 2012. Resistant *Fusarium* keratitis progressing to endophthalmitis. Eye Contact Lens **38:**331–335.
13. **McDermott AM.** 2009. Antimicrobial peptides, p 357–401. *In* Howl J, Jones S (ed). Bioactive peptides. CRC Press, London, United Kingdom.
14. **Steinstraesser L, Kraneburg U, Jacobsen F, Al-Benna S.** 2011. Host defense peptides and their antimicrobial-immunomodulatory duality. Immunobiology **216:**322–333.
15. **Aerts AM, François IE, Cammue BP, Thevissen K.** 2008. The mode of antifungal action of plant, insect and human defensins. Cell. Mol. Life Sci. **65:**2069–2079.
16. **Vylkova S, Nayyar N, Li W, Edgerton M.** 2007. Human beta-defensins kill *Candida albicans* in an energy-dependent and salt-sensitive manner without causing membrane disruption. Antimicrob. Agents Chemother. **51:**154–161.
17. **den Hertog AL, van Marle J, van Veen HA, Van't Hof W, Bolscher JG, Veerman EC, Nieuw Amerongen AV.** 2005. Candidacidal effects of two antimicrobial peptides: histatin 5 causes small membrane defects, but LL-37 causes massive disruption of the cell membrane. Biochem. J. **388:**689–695.
18. **van der Weerden NL, Hancock RE, Anderson MA.** 2010. Permeabilization of fungal hyphae by the plant defensin NaD1 occurs through a cell wall-dependent process. J. Biol. Chem. **285:**37513–37520.
19. **López-García B, Lee PH, Yamasaki K, Gallo RL.** 2005. Antifungal activity of cathelicidins and their potential role in *Candida albicans* skin infection. J. Investig. Dermatol. **125:**108–115.
20. **De Yang Chen Q, Schmidt AP, Anderson GM, Wang JM, Wooters J, Oppenheim JJ, Chertov O.** 2000. LL-37, the neutrophil granule-and epithelial cell derived cathelicidin, utilizes formyl peptide receptor-like 1 (FPRL1) as a receptor to chemoattract human peripheral blood neutrophils, monocytes, and T cells. J. Exp. Med. **192:**1069–1074.
21. **Yang D, Chertov O, Oppenheim JJ.** 2001. Participation of mammalian defensins and cathelicidins in anti-microbial immunity: receptors and activities of human defensins and cathelicidin (LL-37). J. Leukoc. Biol. **69:**691–697.
22. **McDermott AM.** 2009. The role of antimicrobial peptides at the ocular surface. Ophthalmic Res. **41:**60–75.
23. **Huang LC, Reins RY, Gallo RL, McDermott AM.** 2007. Cathelicidin-deficient ($Cnlp^{-/-}$) mice show increased susceptibility to *Pseudomonas aeruginosa* keratitis. Investig. Ophthalmol. Vis. Sci. **48:**4498–4508.
24. **Wu M, McClellan SA, Barrett RP, Zhang Y, Hazlett LD.** 2009. Beta-defensins 2 and 3 together promote resistance to *Pseudomonas aeruginosa* keratitis. J. Immunol. **183:**8054–8060.
25. **Wu M, McClellan SA, Barrett RP, Hazlett LD.** 2009. β-Defensin-2 promotes resistance against infection with *P. aeruginosa*. J. Immunol. **182:**1609–1616.
26. **Kolar SS, McDermott AM.** 2011. Role of host-defence peptides in eye diseases. Cell. Mol. Life Sci. **68:**2201–2213.
27. **Yuan X, Hua X, Wilhelmus KR.** 2010. The corneal expression of antimicrobial peptides during experimental fungal keratitis. Curr. Eye Res. **35:**872–879.
28. **Gao N, Kumar A, Guo H, Wu X, Wheater M, Yu F-S.** 2011. Topical flagellin mediated innate defence against *Candida albicans* keratitis. Investig. Ophthalmol. Vis. Sci. **52:**3074–3082.
29. **Hume EB, Flanagan J, Masoudi S, Zhu H, Cole N, Willcox MD.** 2009. Soft contact lens disinfection solution efficacy: clinical *Fusarium* isolates vs ATCC 36031. Optom. Vis. Sci. **86:**415–419.
30. **Wu TG, Keasler VV, Mitchell BM, Wilhelmus KR.** 2004. Immunosuppression affects the severity of experimental *Fusarium solani* keratitis. J. Infect. Dis. **190:**192–198.
31. **Nizet V, Ohtake T, Lauth X, Trowbridge J, Rudisill J, Dorschner RA, Pestonjamasp V, Piraino J, Huttner K, Gallo RL.** 2001. Innate antimicrobial peptide protects the skin from invasive bacterial infection. Nature **414:**454–457.
32. **Sun Y, Chandra J, Mukherjee P, Szczotka-Flynn L, Ghannoum MA, Pearlman E.** 2010. A murine model of contact lens-associated *Fusarium* keratitis. Investig. Ophthalmol. Vis. Sci. **51:**1511–1516.
33. **Cole N, Hume E, Khan S, Krockenberger M, Thakur A, Husband AJ, Willcox MD.** 2005. Interleukin-4 is not critical to pathogenesis in a mouse model of *Pseudomonas aeruginosa* corneal infection. Curr. Eye Res. **30:**535–542.
34. **Sun Y, Pearlman E.** 2009. Inhibition of corneal inflammation by the TLR4 antagonist Eritoran tetrasodium (E5564). Investig. Ophthalmol. Vis. Sci. **50:**1247–1254.
35. **Wu TG, Wilhelmus KR, Mitchell BM.** 2003. Experimental keratomycosis in a mouse model. Investig. Ophthalmol. Vis. Sci. **44:**210–216.
36. **Tarabishy AB, Aldabagh B, Sun Y, Imamura Y, Mukherjee PK, Lass JH, Ghannoum MA, Pearlman E.** 2008. MyD88 regulation of *Fusarium* keratitis is dependent on TLR4 and IL-1R1 but not TLR2. J. Immunol. **181:**593–600.
37. **Shin SY, Kang SW, Lee DG, Eom SH, Song WK, Kim JI.** 2000. CRAMP analogues having potent antibiotic activity against bacterial, fungal, and tumor cells without hemolytic activity. Biochem. Biophys. Res. Commun. **275:**904–909.
38. **Jiang Y, Yi X, Li M, Wang T, Qi T, She X.** 2012. Antimicrobial activities of recombinant mouse β-defensin 3 and its synergy with antibiotics. J. Mater. Sci. Mater. Med. **23:**1723–1728.
39. **Kurosaka K, Chen Q, Yarovinsky F, Oppenheim JJ, Yang D.** 2005. Mouse cathelin-related antimicrobial peptide chemoattracts leukocytes using formyl peptide receptor-like 1/mouse formyl peptide receptor-like 2 as the receptor and acts as an immune adjuvant. J. Immunol. **174:**6257–6265.